Multiwalled Carbon Nanotube Purification Probed by Electrochemistry: Low-Temperature Chlorine Gas Treatment Meets High-Temperature Annealing

Nawal Berrada, Wassim El Housseini, Alexandre Desforges, Jérôme Gleize, Jaafar Ghanbaja, Mathieu Etienne, Matthieu Houllé, Christine Bellouard, Brigitte Vigolo

Multiwalled carbon nanotube purification probed by electrochemistry: low temperature chlorine gas treatment meets high temperature annealing

Nawal Berrada,[a] Wassim El Housseini,[b] Alexandre Desforges,[a] Jérôme Gleize,[c] Jaafar Ghanbaja,[a] Mathieu Etienne,[b] Matthieu Houllé,[d] Christine Bellouard,[a] Brigitte Vigolo,*[a]

[a] Dr. Nawal Berrada, N. B., Dr. Alexandre Desforges, A. D., Dr. Jaafar Ghanbaja, J. G., Dr. Christine Bellouard, C. B., Dr. Brigitte Vigolo, B. V.
Université de Lorraine, CNRS, IJL, F-54000 Nancy, France
E-mail: Brigitte.Vigolo@univ-lorraine.fr
[b] Mr. Wassim El Housseini, W. E. H., Dr. Mathieu Etienne, M. E.
Université de Lorraine, CNRS, LCPME, F-54000 Nancy, France
[c] Dr. Jérôme Gleize, J. G.
Université de Lorraine, LCP-A2MC, F-57000 Metz, France
[d] Dr. Matthieu Houllé, M. H.
Nanocyl S.A. 4, Rue de l'Essor, 5060 Sambreville, Belgique

Supporting information for this article is given via a link at the end of the document.

Abstract: The metal-based residues in carbon nanotube samples can have an enormous impact to their properties which hinders their transfer to practical applications. Development of high-performance purification methods and high sensitive approaches to detect and quantify the remaining impurities within the nanotube samples are still an active research field. Here, commercial multiwalled carbon nanotubes have been purified thanks to a non-standard one-step gas phase treatment using chlorine. Its facile reaction with the metal based impurities located inside and outside the carbon nanotubes allows to efficiently remove them at 1000 °C, with a sample yield of 79 %. Raman spectroscopy and X-ray photoelectron spectroscopy show that the carbon nanotube quality is preserved after purification. The quantity of magnetic residues is accurately evaluated by magnetic measurements, their outcome content is below 500 ppm (weight %). Finally, the redox behavior probed with hydrogen peroxide reduction is competitive with that obtained with a commercial sample thermally purified at 2400 °C. These two techniques were combined for the first time for high sensitivity characterization of ultra-pure multiwalled carbon nanotubes. The used chlorine - based treatment fulfills the requirements of an alternative tool to develop low energy processes for large scale industrial production of purified carbon nanotubes.

Introduction

Due to their unique structure, carbon nanotubes (CNTs) offer a combination of remarkable properties and they fascinate scientists since they can be used in a wide range of applications. CNTs are nanostructured all-carbon tubes with high surface area; they are light and they possess excellent electrical and thermal conductivity along with superior mechanical properties [1,2]. Their bulk production is commonly achieved thanks to chemical vapor deposition (CVD) and arc discharge [3,4]. Catalytic CVD or CCVD is more suitable to produce multi-walled CNTs (MWCNTs) in high amount since such technique is compatible with continuous synthesis processes [5]. However, the as-produced MWCNT powders by CCVD usually do not contain just CNTs but also other carbonaceous particles such as amorphous carbon, fullerenes, nanocrystalline graphite and metallic particles from the used catalysts and/or catalyst supports. By optimizing the synthesis conditions, the carbonaceous byproducts can be efficiently eliminated even from MWCNTs produced in large amount. On the contrary, catalyst residue impurity cannot be avoided; they are indeed involved in the CNT growth mechanism itself by CVD [6]. These metallic particles are non-desired since they are responsible of lessening the CNT properties and their impact cannot be clearly identified and discriminated from that induced by the CNTs themselves [7,8]. The presence of these metallic impurities hinders development of well-controlled and robust CNT-based materials and devices. This is the reason why efficient elimination of these metal-based residues is highly desired [9–11]. And since their amount is very low within the purified CNT samples, their detection and quantification are difficult and require specific approaches and techniques[12–14]. Due to the increased role of CNTs in electrochemistry involved in energy and environmental applications, it is of great interest to investigate their electrochemical behavior. Such investigation is all the more important because electrocatalytic activity of CNT samples has been shown to be affected by carbon [15,16] and metallic impurities even at very weak content [17–19]. Electrochemistry furnishes then as well a highly sensitive detection probe.

Because the catalysts and their supports are difficult to remove, intensive treatments are required to produce purified CNTs. However, these approaches, based on liquid phase treatments in strong acids (nitric, sulfuric acid…) and/or oxidants (potassium permanganate, hydrogen peroxide…), affect the quality of the CNTs and the purification sample yield, *i.e.* the amount of the outcome purified CNTs with respect to that of the raw CNTs is weak. Moreover, these approaches are multi-step and time consuming. They are then not competitive for further scale-up transfer, as they cannot fulfill the yield, time and quality constraints. High temperature thermal annealing under vacuum or inert gas matches with these requirements since the metal particles are vaporized at 2000 – 2500 °C and the CNTs do not suffer of any damaging by chemicals [20,21]. However, these methods require high energy consumption processes due to the high temperature range used.

Lower-temperature gas-phase approaches have been proposed in literature. Interestingly, the sublimation temperature of the metal-based impurities can be significantly reduced in the 800-1200 °C range after their facile reaction with halogens such as bromine [22] or chlorine [23,24]. Moreover, since halogens are advantageously poorly reactive with carbon, the CNTs can hence be preserved or even protected by such treatments [25]. We have already applied such chlorine-based purification to single walled CNTs (SWCNTs) from several sources and double-walled CNTs (DWCNTs) with good purification yields [13,23,26–28]. Because of well protected metallic impurities within carbon species in CNT samples, further enhancement in metallic removal yield has been only possible by adding O_2 in Cl_2 in a narrow condition window[26]. MWCNTs are the preferred CNT type since they can be synthetized in amount suitable for upscaling approach.

We propose here to purify MWCNTs produced by Nanocyl S.A. by the home-developed patented one-step chlorine-based purification method[29]. Efficiency and performance of this method are put in competition with a high temperature thermal treatment performed by the MWCNT supplier. Such high temperature treatment suffer of high energy consumption. In a first step of the study, metal-based residues are roughly quantified by thermogravimetric analysis (TGA). The overall quality of the samples is investigated by transmission electron microscopy (TEM), X-ray photoelectron spectroscopy (XPS) and Raman spectroscopy. After these standard complementary characterizations, magnetic and electrochemical measurements have been performed to go a step further and to deal with the very low content of metal impurities in MWCNTs. To the best of our knowledge, these two techniques have never been combined as highly sensitive tools for CNT purification investigation.

Results and discussion

The one-step gas phase purification treatment applied consists of heating the raw MWCNT powder placed in a tubular oven in a chlorine/nitrogen flow (Scheme 1). During temperature raise and dwell, metal chlorides are formed and sublimated at high temperature inside the oven. They are then entrained by the gas stream and they naturally deposit at the nearest cold location of the set-up, out of the oven; each metal chloride corresponding then to a type of metal (Co, Fe, Al) impurity present in the MWCNT sample [30,31]. They hence appear on the internal surface of the silica tube with a specific color (Scheme 1).

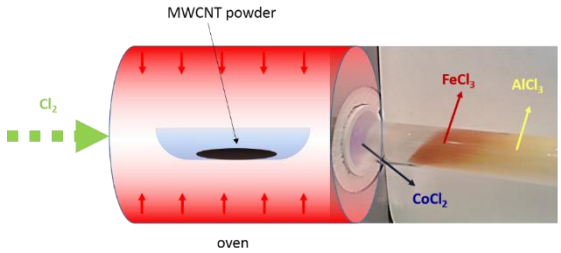

Scheme 1 Scheme-photo combination illustrating the purification process occurring with the visual appearance of the three metal chlorides (each with its specific color) formed from each kind of metal impurity present in the raw MWCNT sample.

The respective nature of each metal chloride can be visually recognized: blue for cobalt chloride ($CoCl_2$), red for iron chloride ($FeCl_3$) and yellow for aluminum chloride ($AlCl_3$). The respective location of each deposited chloride is related to its sublimation temperature. The higher its sublimation temperature, the closer to the oven the deposit. The expected sublimation temperatures are 500, 316 and 187 °C for (bulk) $CoCl_2$, $FeCl_3$ and $AlCl_3$, respectively.

Table 1 summarizes the main steps of the purification method applied to the MWCNT samples and reports the sample yield of the used treatments. The sample yield is defined as the ratio of the mass of the outcome purified sample with respect to the income total mass of raw sample. The chlorine based treatment pCl2 provides a high sample yield of the order of 80 %, close to that of pHT.

Table 1 Main treatment steps, sample yields and quantified residues in the raw and the purified MWCNT samples from TGA.

Samples	raw	pHT	pCl1	pCl2
Treatment	-	Vacuum 240 min 2400 °C	$Cl_2 + N_2$ 40 min 1000°C N_2 120 min 1100°C	$Cl_2 + N_2$ 120 min 1000°C N_2 120 min 1000°C
Sample Yield (%)	-	85	N.A.	79
TGA (%)	10.4	≤ 0.5	≤ 0.5	≤ 0.5

Figure 1 shows the thermograms of the raw and the purified MWCNT samples, quantification of the residues from TGA is given in Table 1.

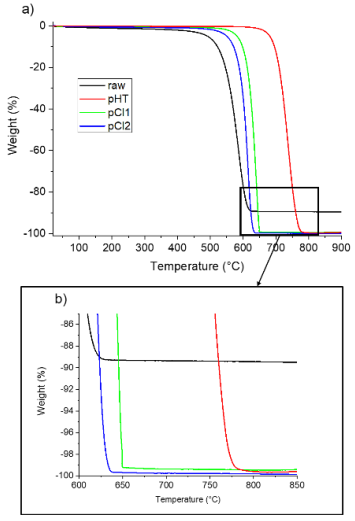

Figure 1 a) Thermograms of the raw MWCNTs (raw in black) and the purified MWCNTs: pHT in red, pCl1 in green and pCl2 in blue; b) zoom of the high temperature range of the thermograms.

In figure 1, the main weight loss due to MWCNT combustion occurs at around 580 °C for the raw sample. The MWCNT combustion temperature is upshifted up to the 610-630 °C range for the MWCNTs purified with chlorine as usually observed in CNT samples which contain a reduced amount of metal-based impurities [32]. After purification at 2400°C (pHT), the metal-based impurity content is diminished from 10.4 wt.% (raw) down to a value lower than 0.5 %. The impurity contents obtained with both chlorine-based treatments are found in the same range, revealing their high efficiency. In this range, the accuracy of TGA is indeed not suitable to provide a reliable impurity content quantification. As a consequence, much more sensitive techniques such as magnetic and redox investigations will be presented in the next section.

TEM observations performed on the raw sample show the absence of amorphous carbon and they put into evidence some metallic impurities located inside the inner channel of the tubes (figure 2a). In such case, their accessibility by a gas as chlorine is certainly much more favored than for a liquid phase treatment, as confirmed by the low TGA residue contents in the purified MWCNTs. Figures 2b and 2c show TEM images of pCl2 in which no more metallic impurities/dark particles are visible in contrary to what is observed in the raw MWCNTs (figure 2a). Low magnification TEM observation does not show any evidence of the presence of metal-based impurities in pCl2 (figure S1, Supporting Information). At high magnification, the parallel straight lines, *i.e.* the MWCNT walls, are well noticeable without any perceptible damaging subsequent to the purification treatment.

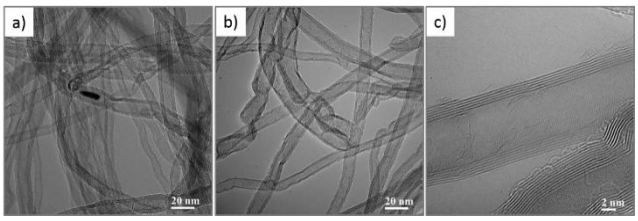

Figure 2 Typical TEM bright field micrographs of a) raw and b) and c) of pCl2.

XPS is widely carried out to analyze the surface chemistry of CNTs. The wide range XPS spectra for raw, pHT, pCl1 and pCl2, the Cl 2p XPS features of pCl1 and pCl2 and their respective decomposition are presented in Supporting Information, section 2, in figures S2 and S3, respectively. No evidence of metal presence is visible in the XPS signals of the raw and purified MWCNTs. Table 2 gathers the atomic contents of carbon, oxygen and chlorine in the studied MWCNT samples from XPS.

In terms of composition, all the samples show high carbon content around 98-99 at.%. The oxygen content is roughly in the 0.5-1 at.% range for the raw and the treated samples. As already reported from our previous works [25,33], chlorine could be detected in MWCNTs purified by the chlorine-based method. For both pCl1 and pCl2, the Cl 2p feature typically shows two components (each consisting of the 3/2 and 1/2 level with a spin−orbit splitting of 1.6 eV) as shown in figure S3 (Supporting Information). The high-energy contribution with the Cl 2p3/2 component at around 200.10-200.15 eV is attributed to C-Cl bonds [33]. No contribution at lower energy that could be assigned to metal-chlorine is detected.

The C 1s spectra of all samples are shown in figure S4 in Supporting Information. All spectra are almost superimposed, showing that the carbon atom environment of the MWCNTs are not modified by functionalization after any of the purification treatments.

Two contributing peaks (at 284.6 eV and around 290 eV) readily attributed to the sp^2 and $\pi - \pi*$ components are clearly observed, others contributions are however present, but give rise only to a light shoulder of the strong sp^2 signal. The analysis of this signal is presented in figure S5 (Supporting Information).

Table 2 Relative atomic contents of carbon, oxygen and chlorine (with their contributions) from XPS analysis.

sample	C at.%	O at.%	Cl at.%	Cl 2p contributions
raw	99.23	0.77	0	- -
pHT	99.37	0.63	0	- -
pCl1	99.03	0.54	0.43	200.10 eV (C-Cl bonds) and 201.68 eV (spin-orbit coupling)
pCl2	98.37	1.12	0.51	200.15 eV (C-Cl bonds) and 201.73 eV (spin-orbit coupling)

Four components typically observed in carbon nanomaterials have been considered: i) carbon sp^2 corresponding to the C=C bonds belonging to the MWCNT framework, ii) carbon hybridized sp^3, iii) carbon-oxygen bond contribution in the 286 – 290 eV range and iv) $\pi - \pi*$ contribution being the characteristic shake-up line found in aromatic compounds. The contribution of the C-Cl bonds in pCl1 and pCl2 is expected to be found in the 287.0-287.2 eV range meaning that it cannot be distinguished from that of the C-O contribution. And since the number of C-O or C-Cl bonds is weak, XPS decomposition reliability is based on the use of only one component for the carbon atoms linked to either O or Cl. Figure 3 gives the respective concentrations for each component based on the C 1s feature decompositions shown in figure S5 (Supporting Information).

For all samples, the 4 components contribute equally of the C 1s peak, in agreement with the already mentioned similarity between the raw and the treated MWCNT samples. C 1s sp^2 and sp^3 components contribute for 56-62 % and 17-21 % of the C 1s signal, respectively. The component around 287 eV corresponds to the presence of native or introduced functional groups containing oxygen or chlorine to the MWCNT surface, it contributes to only 8-11 % of the C 1s signal.

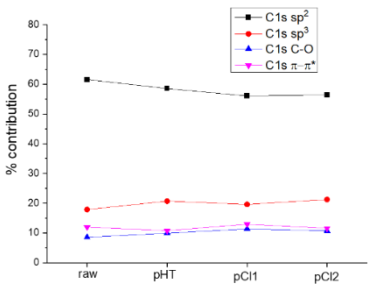

Figure 3 Relative contributions from C 1s decomposition from XPS for raw, pHT, pCl1 and pCl2.

Figure 4 shows I_D/I_G ratios from Raman spectroscopy of the raw and the treated MWCNTs (typical spectra are shown in Supporting Information, section 2, figure S6). Intensity of D band is related to the structural defects in nanotubes and I_D/I_G is known to increase when defects are introduced within the graphitic structure of the CNTs.

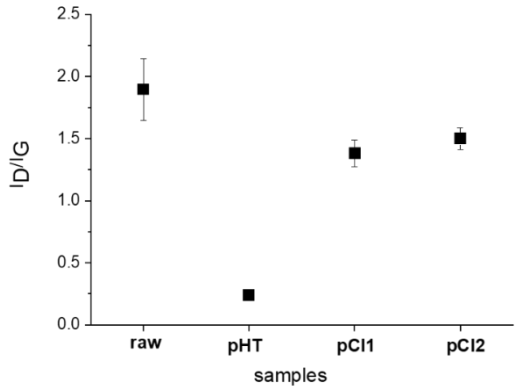

Figure 4 I_D/I_G from Raman spectroscopy of the studied MWCNT samples: raw, pHT, pCl1 and pCl2.

Compared to the raw MWCNTs, a significant decrease in I_D/I_G ratio is observed in figure 4 for pHT due to the high temperature used, 2400 °C (I_D/I_G = 1.9 ± 0.2 for raw and I_D/I_G = 0.24 ± 0.01 for pHT). Concerning the treatments using chlorine, I_D/I_G remains similar after treatment, meaning that the MWCNT structural quality is undoubtedly preserved, I_D/I_G being of 1.4 ± 0.1 and 1.5 ± 0.1 for pCl1 and pCl2, respectively.
As a conclusion, the chemical characteristics of the MWCNTs appear unchanged after all the applied purification treatments. Their structural properties are significantly improved after the high temperature treatment and they are well preserved in case of the chlorine-based treatments. In the following, the study is focused on the metal-based impurity analysis.

The raw MWCNT sample exhibits at 300 K a ferromagnetic behavior as shown in figure 5a. The signal contains indeed also a superparamagnetic component as illustrated by the temperature dependence of the field cooled-zero field cooled (FC-ZFC) magnetization presented in figure S7 (Supporting Information, section 4). Anyway, the magnetization saturates close to 0.75 emu/g at 300 K (figure 5a), in agreement with previously reported magnetic measurements [34]. For an expected Fe or Co oxide content below 1 %, that corresponds to a mean magnetization per gram of magnetic compounds of the order of 75 emu/g. This low magnetization is in agreement with the presence of iron and cobalt oxide magnetic nanoparticles which can be ferri- or ferromagnetic (around 80-100 emu/g) or antiferromagnetic (0 emu/g). At 5 K, a large increase in magnetization is observed with increasing field, without saturation. As no phase transition is observed under low field conditions (figure S7, Supporting Information, section 4), this behavior is attributed to paramagnetic or disordered moments (at the periphery of nanoparticles for instance).

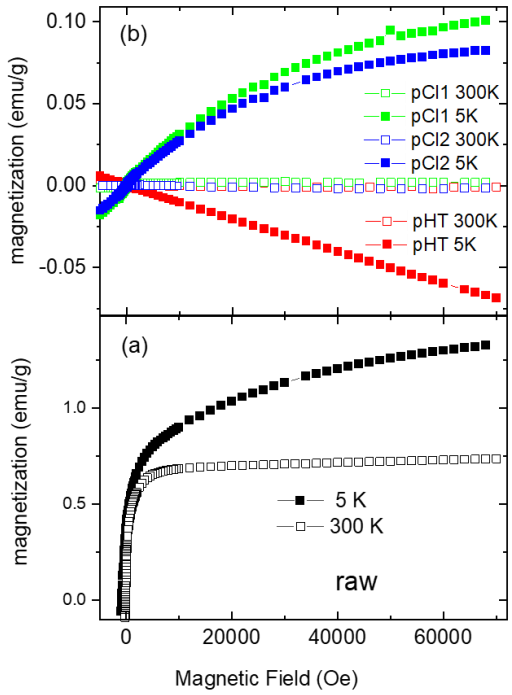

Figure 5 Field dependence of the magnetization at 5 K and 300 K of the raw sample (a) and of the purified samples (b).

The field dependence of the magnetization for the purified samples, after correction by the room temperature diamagnetic slope, is plotted in figure 5b. We point out that the scale is about one order of magnitude below that used in figure 5a. One can observe that the room temperature ferromagnetic signal has disappeared in the case of pHT and pCl2. A weak ferromagnetic (or superparamagnetic) contribution, of the order of 0.2-0.3 % of that found for the raw sample is only detected in pCl1. Within the assumption of a maximum of 1 wt.% of magnetic metals in “raw”, this ferromagnetic (or superparamagnetic) component corresponds to a residual content of magnetic species below 0.003 wt.%. These results are in total agreement with the low residual content found by TGA (Table 1).
At 5 K, the field dependence of the pHT sample remains perfectly linear, indicating the complete absence of magnetic impurities. On the contrary, a magnetic signal is clearly detected at 5 K after the chlorine-based treatments. Moreover, FC-ZFC measurements performed below 30 K for these purified MWCNT samples, exhibit a hysteresis below about 10 K, and a maximum of the ZFC curve around 5 K, as shown in figure S8 (Supporting Information). The absence of such features in the raw sample allows to attribute this low temperature signal to the compounds formed by reaction with Cl_2 such as $FeCl_3$ or $CoCl_2$. Moreover, these compounds show some phase transitions at low temperature (< 30 K) when intercalated in graphite layers [35,36]. We recall that some chlorine-containing compounds have been clearly found after similar Cl_2 treatment of SWCNTs without final N_2 cleaning step [13]. Above 20 K, no irreversibility is observed, the magnetic signal of the chlorine treated samples is paramagnetic. The temperature dependence of the

magnetization measured under 10 kOe can be fitted (figure 6) with a Curie-Weiss law as:

$$M(T,H) = d + \frac{C}{T-\theta} H \qquad (1)$$

"d" is a constant arising mainly from the diamagnetic contribution of the nanotubes which is assumed independent of temperature in the 20 K-120 K range, "C" is the Curie constant and "θ" characterizes the interactions between magnetic moments. The parameters provided by the fits are reported in Table S1 (Supporting Information). The positive θ value around 7 K indicates ferromagnetic interactions. This value is much lower than those occurring in pure $CoCl_2$ or $FeCl_3$ (in the order if 40-60 K), the possibility of residual $CoCl_2$ or $FeCl_3$ grains is then ruled out. As the Curie-Weiss temperature of intercalated $FeCl_3$ is negative [37], the paramagnetic signal is rather attributed to intercalated $CoCl_2$, with presents in-plane ferromagnetic interactions [38].

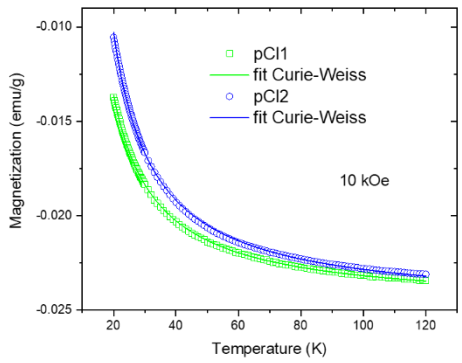

Figure 6 Temperature dependence of the magnetization measured under 10 kOe and fitted with equation 1 as described in the text for pCl1 and pCl2 samples.

The paramagnetic impurity weight ratios, considering Co^{2+} species, with an effective moment of $4.8\,\mu_B$, are reported in Table S1. The total magnetic mass ratios, considering paramagnetic and ferromagnetic (or superpamagnetic) contributions, are also reported. As a conclusion, the mass concentration of the magnetic species remaining as byproducts is roughly 4.10^2 ppm. Moreover, the magnetic study has shown that no magnetic impurity can be detected in the pHT sample, and that all magnetic impurities have been attacked by Cl_2 for the pCl2 process.

The electrochemical response of the purified MWCNTs was evaluated through cyclic voltammetry at a scan rate of 5 mV/s. Figure 7 exhibits the electrochemical reduction of 5 mM H_2O_2 on the used MWCNTs that have been deposited on a glassy carbon electrode without CNTs (dashed line): raw (black line), pHT (red line), pCl1 (green line) and pCl2 (blue line).

Figure 7 Cyclic voltammograms resulting from the electrochemical reduction of 5 mM H_2O_2 at glassy carbon electrodes modified with the used MWCNTs: raw (black line), pHT (red line), pCl1 (green line), pCl2 (blue line), and without CNT (black dashed line). Conditions: scan rate, 5 mV/s; cycle 3; background electrolyte, 100 mM KCl; pH 6.9.

Without CNT, a negligible reduction of H_2O_2 is observed on glassy carbon electrode (GCE), showing only -3 µA at -0.9 V vs Ag/AgCl (3 M). In contrast, a significant reduction of H_2O_2 on the raw MWCNTs modified GCE is observed from about -0.2 V and reaches a high current in the order of -63 µA at -0.9 V that can be compared to the results reported in literature using MWCNTs with Fe (III) especially Fe_3O_4 [19,39], in agreement with the presence of Fe as declared by the supplier of the raw MWCNT sample used.

H_2O_2 reduction in the presence of pHT (red curve) is far lower than what is observed for the raw MWCNTs, reaching only -9 µA at -0.9 V, but still increased by comparison to bare GCE. This result is somehow in agreement with the magnetic measurements, where absolutely no magnetic signal arising from impurities is detected. However, it is not clear here if this H_2O_2 signal is due to remaining impurities not detectable with other analytical techniques or only caused by the increased electroactive surface area from the MWCNT layer. The purification treatment under chlorine applied during only 40 min (green curve) provides electrochemical properties in between raw and pHT. pCl1 behavior shows a reduction current of -34 µA at -0.9 V. Magnetic measurements have shown that a residual ferromagnetic signal is detected at 300 K in this sample. The remaining residues which may also contain some nonmagnetic alumina give then rise to a reduction current which is more than three times the current value found for pHT.

Finally, pCl2, which has been treated during 120 min under chlorine presents a response comparable to that of pHT, reaching only -11 µA at -0.9 V. As a consequence, the Cl_2 treatment at 1000 °C during 120 min leads to electrochemical properties competing with the 2400 ° C thermal treatment. That means that the residual byproducts detected through magnetism (weight % ≤ 0.04 %) which have been all attacked by chlorine, and are inserted in carbon layers have no significant impact on the electrochemical behavior.

Conclusion

Commercial MWCNTs were purified by a one-step gas phase treatment by using chlorine at 1000 °C. The metal-based impurities are efficiently eliminated leading to a residual content determined by TGA at the limit of the confidence threshold (lower or equal to 0.5 %). According to our knowledge, for the first time, two complementary highly sensitive techniques have

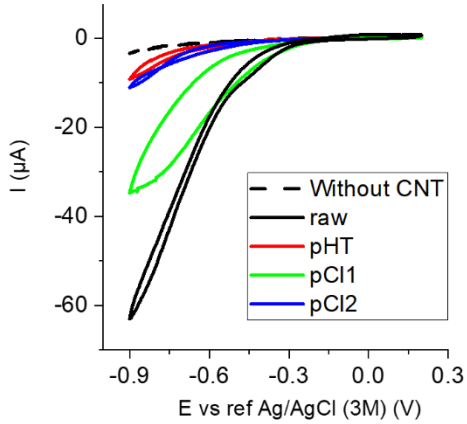

then been investigated: magnetic measurements and electrochemistry with H_2O_2 reduction as probe reaction. Our optimized purification conditions provide a sample with only 0.04 wt.% residual magnetic species intercalated in carbon sheets. This sample exhibits then an electrochemical behavior in close competition with a reference sample provided by the supplier where no magnetic impurity is detected. Beyond this peculiar results, we have demonstrated that electrochemistry and magnetism analysis can be successfully combined for a fine understanding of the mechanism and efficiency of purification. Such approach can also be applied to other carbon nanomaterial investigation.

Focusing on the purified CNTs, the proposed chlorine-based treatment undeniably preserves the chemical and structural quality of the carbon nanotubes as shown by XPS and Raman spectroscopy respectively. From a quantitative point of view, the sample yield is close to the yield of standard high-temperature treatment by the supplier. Finally, the relatively low temperature, 1000 °C, of our treatment compared to the high-temperature annealing by the supplier, at 2400 °C, with the same duration, offers a subsequent energy saving. As a consequence, the proposed chlorine-based treatment opens the way of an alternative tool for large scale industrial production and low energy consumption.

Experimental Section

Potassium permanganate ($KMnO_4$) was purchased from Alfa Aesar, sodium hydroxide (NaOH) from VWR and sulfuric acid (H_2SO_4) 95-97 % and hydrochloric acid (HCl) 37 % were provided by Sigma Aldrich. The used raw MWCNT sample (NC7000) and a thermally purified MWCNT sample (NX7100 – ultra-purified MWCNTs) were kindly provided by Nanocyl S.A., Belgium. From the supplier information, the inorganic impurities in the NC7000 MWCNT are Al_2O_3 (around 9 wt.%) and Fe and Co oxides (< 1 wt.%). The treatment providing the thermally purified MWCNTs consists in a vacuum annealing at 2400 °C during 4 h, and this reference sample is referred to as “pHT” in the following.

In the present work, the raw MWCNTs (referred to as “raw”) are purified by a chlorine-based treatment using an experimental set-up described elsewhere [21]. In comparison with previous studies [18,20,21], the duration and rate of the chlorine flow have been optimized in order to minimize the metallic impurity content and a subsequent annealing step under nitrogen has been added in order to minimize the chlorine content in the treated MWCNT. The raw MWCNT powder (typically 250 mg) is loaded in a silica boat (length 10 cm, width 1 cm) and transferred into a tubular oven (scheme 1). Temperature is raised at 10 °C/min to reach the chosen treatment temperature (1000°C or 1100°C) which is maintained during a certain period. Chlorine is produced *in situ* by oxidation of HCl 12N by $KMnO_4$ (powder form). HCl is fed drop-by-drop into a reaction balloon containing $KMnO_4$. The formed chlorine is purified by successive flasks of concentrated H_2SO_4 9N and calcium chlorine ($CaCl_2$) to remove remaining HCl and H_2O. The chlorine flow rate evaluated from the consumed HCl is of 150 mL/min. The carrier gas is nitrogen (N_2). After the chosen treatment duration, the HCl drop-by-drop is stopped and the thermal treatment is continued under N_2 alone. The entire process consists then of a one-step method. Thereafter, each purified powder is left naturally cooling down under N_2 flow.

The sample named “pCl1” was treated under chlorine at 1000 °C for 40 min followed by 120 min under nitrogen at 1100 °C. “pCl2” was submitted to chlorine at 1000°C for 120 min followed by 120 min under nitrogen at 1000°C.

Transmission electron microscopy (TEM) observations were done by means of using a JEOL ARM 200F cold field-emission electron gun (FEG) (operating voltage of 80 kV). The MWCNT powder was gently dispersed in a sonication bath and the prepared MWCNT dispersion was then deposited on a TEM holey carbon grid, 200 mesh. For each sample, at least 25-30 images were observed and analyzed for many zones on the TEM grid; the shown TEM images are typical and present the general aspect of each sample.

Thermogravimetric analysis (TGA) was carried out with a Setaram Setsys evolution 1750 Thermal Gravimetric Analyser. The carrier gas, a reconstituted dry air, was first flowed for 1 h before raising temperature from room temperature to 900 °C at 5 °C/min (air flow rate 20 mL/min). The raw data were corrected by subtracting a blank curve corresponding to the weight variation of the empty platinum crucible subjected to the same temperature ramp than that used for the samples.

A LabRAM HR 800 micro-Raman spectrometer (incident wavelength 632.8 nm, power 0.25 mW/μm^2) was used for Raman spectroscopy investigations. For each sample, at least three spectra were recorded on different areas to ensure a good reproducibility of the analysis. For data analysis, after subtracting a baseline, the I_D/I_G intensity ratio was calculated from the maximum height of the D and the G band for each spectrum.

X-ray photoelectron spectroscopy spectra were collected on a Kratos Axis Ultra (Kratos Analytical, UK) spectrometer equipped with a monochromatic Al Kα (1486.6 eV). All spectra were recorded at a 90° takeoff angle. The high-resolution regions were acquired with 0.1 eV step and 20 eV pass energy (instrumental resolution better than 0.5 eV). The main contribution of the C1s signal corresponding to C1s sp^2 was calibrated to 284.6 eV. For the spectrum fitting, a Shirley line is used as background and combined Gaussian (30 %) and Lorentzian (70 %) line profiles are applied to decomposed the XPS signals by Casa XPS software.

Magnetic measurements have been performed with a SQUID-VSM magnetometer from Quantum-Design, in the DC measurement mode. The samples (3-4 mg for purified samples, 6 mg for the raw sample) have been introduced in a gelatin capsule maintained in a plastic straw. The field and temperature dependences of the magnetization have been systematically subtracted by the contribution of sample holder. To focus on the magnetic signal of the residual impurities after treatment, the field dependence of the magnetization of the purified samples measured at 5 K and 300 K have been subtracted by the negative slope fitted at 300 K above 30 kOe (arising from the diamagnetic signal of CNTs).

Cyclic voltammograms were recorded with the Autolab PGSTAT. The working electrode was a glassy carbon electrode (BASi, West Lafayette, USA). The working electrode, the Ag/AgCl reference electrode and a platin wire used as counter electrode were inserted through holes in a glassy cell containing 20 mL of 0.1 M KCl and 5 mM H_2O_2. The pH of the solution was 6.9.

Cyclic voltammograms were recorded between 0.2 V and -0.9 V at a scan rate of 5 mV/s. The CNT sample, dispersed in ethanol, has been exposed to ultrasounds for 5 min then mixed. This process has been repeated 4 times. The surface modification of the working electrode (diameter of 3 mm) was proceeded by casting 5 µL of the solution of each CNT sample in ethanol. The working electrode has been left 15 min until the complete evaporation of ethanol. 15 min before and during cyclic voltammograms, the solution has been bubbled with nitrogen in order to eliminate residual oxygen. Before each experiment, the glassy carbon electrode was polished with 0.05 µm alumina slurries then washed with distilled water.

Acknowledgements

Supported by the « SONOMA» project co-funded by FEDER-FSE Lorraine et Massif des Vosges 2014-2020, a European Union Program. The authors would like to thank L. Aranda for his help for TGA experiment. The authors would like to thank P. Franchetti for his help for Raman spectroscopy. We would like to thank the platform “Microscopies, Microprobes and Metallography (3M)” (Institut Jean Lamour, IJL, Nancy, France). B.V. thanks the platform “Spectroscopies et Microscopies des Interfaces” (Laboratory of Physical Chemistry and Microbiology for Materials and the Environment, LCPME, Nancy, France) and A. Renard, Dr. M. Mallet (LCPME) for XPS analysis. C.B. thanks the platform ”Magnétisme” of the Institut Jean Lamour.

Keywords: Carbon nanotubes • Chlorine • Metallic impurities • Purification • Quantification

Twitter: @labo_IJL and @Univ_Lorraine

References

[1] P. M. Ajayan, O. Z. Zhou, in *Carbon Nanotub Es: Synthesis, Structure, Properties, and Applications* (Eds.: M.S. Dresselhaus, G. Dresselhaus, P.H. Avouris), Springer-Verlag Berlin, Berlin, **2001**, pp. 391–425.
[2] V. N. Popov, *Mater. Sci. Eng.: R: Reports* **2004**, *43*, 61–102.
[3] K. A. Shah, B. A. Tali, *Mater. Sci. Semicond. Process.* **2016**, *41*, 67–82.
[4] N. Arora, N. N. Sharma, *Diam. Relat. Mater.* **2014**, *50*, 135–150.
[5] J. Huang, Q. Zhang, M. Zhao, F. Wei, *Chin. Sci. Bull.* **2012**, *57*, 157–166.
[6] M. Kumar, Y. Ando, *J. Nanosci. Nanotechnol.* **2010**, *10*, 3739–3758.
[7] Q. Yuan, L. Li, Q. Li, F. Ding, *J. Phys. Chem. C* **2013**, *117*, 5470–5474.
[8] M. Pumera, A. Ambrosi, E. L. K. Chng, *Chem. Sci.* **2012**, *3*, 3347–3355.
[9] P.-X. Hou, C. Liu, H.-M. Cheng, *Carbon* **2008**, *46*, 2003–2025.
[10] A. B. Makama, A. Salmiaton, N. Abdullah, T. S. Y. Choong, E. B. Saion, *Sep. Sci. Technol.* **2014**, *49*, 2797–2812.
[11] H. Ribeiro, M. C. Schnitzler, W. M. da Silva, A. P. Santos, *Surf. Interfaces* **2021**, *26*, 101389.
[12] C. Ge, F. Lao, W. Li, Y. Li, C. Chen, Y. Qiu, X. Mao, B. Li, Z. Chai, Y. Zhao, *Anal. Chem.* **2008**, *80*, 9426–9434.
[13] C. Bellouard, G. Mercier, S. Cahen, J. Ghanbaja, G. Medjandi, J. Gleize, G. Lamura, C. Herold, B. Vigolo, *J. Magn. Magn. Mater.* **2016**, *411*, 39–48.
[14] E. Pellicer, A. B. González-Guerrero, J. Nogués, L. M. Lechuga, E. Mendoza, *Carbon* **2009**, *47*, 758–763.
[15] L. Wang, A. Ambrosi, M. Pumera, *Anal. Chem.* **2013**, *85*, 6195–6197.
[16] E. J. E. Stuart, M. Pumera, *J. Phys. Chem. C* **2011**, *115*, 5530–5534.
[17] C. Batchelor-McAuley, G. G. Wildgoose, R. G. Compton, L. Shao, M. L. H. Green, *Sens. Actuators B-Chem.* **2008**, *132*, 356–360.
[18] J. Kruusma, N. Mould, K. Jurkschat, A. Crossley, C. E. Banks, *Electrochem. Commun.* **2007**, *9*, 2330–2333.
[19] B. Sljukic, C. E. Banks, R. G. Compton, *Nano Lett.* **2006**, *6*, 1556–1558.
[20] R. Andrews, D. Jacques, D. Qian, E. C. Dickey, *Carbon* **2001**, *39*, 1681–1687.
[21] W. Huang, Y. Wang, G. H. Luo, F. Wei, *Carbon* **2003**, *41*, 2585–2590.
[22] S. Zarska, D. Kulawik, J. Drabowicz, W. Ciesielski, *Fuller. Nanotub. Carbon Nanostruct.* **2017**, *25*, 563–569.
[23] G. Mercier, C. Herold, J.-F. Mareche, S. Cahen, J. Gleize, J. Ghanbaja, G. Lamura, C. Bellouard, B. Vigolo, *New J. Chem.* **2013**, *37*, 790–795.
[24] E. L. K. Chng, H. L. Poh, Z. Sofer, M. Pumera, *Phys. Chem. Chem. Phys.* **2013**, *15*, 5615–5619.
[25] N. Berrada, A. Desforges, C. Bellouard, E. Flahaut, J. Gleize, J. Ghanbaja, B. Vigolo, *J. Phys. Chem. C* **2019**, *123*, 14725–14733.
[26] N. Berrada, S. Hamze, A. Desforges, J. Ghanbaja, J. Gleize, T. Maré, B. Vigolo, P. Estellé, *J. Mol. Liq.* **2019**, *293*, 111473.
[27] A. Desforges, A. V. Bridi, J. Kadok, E. Flahaut, F. Le Normand, J. Gleize, C. Bellouard, J. Ghanbaja, B. Vigolo, *Carbon* **2016**, *110*, 292–303.
[28] E. Remy, S. Cahen, B. Malaman, J. Ghanbaja, C. Bellouard, G. Medjahdi, A. Desforges, S. Fontana, J. Gleize, B. Vigolo, C. Herold, *Carbon* **2015**, *93*, 933–944.
[29] G. Mercier, J.-F. Mareche, S. Cahen, C. Herold, B. Vigolo, *Purifying Carbon* Nanotubes, Patentt WO2012056184A3 **2012**.
[30] A. J. Taylor-Just, M. D. Ihrie, K. S. Duke, H. Y. Lee, D. J. You, S. Hussain, V. K. Kodali, C. Ziemann, O. Creutzenberg, A. Vulpoi, F. Turcu, M. Potara, M. Todea, S. van den Brule, D. Lison, J. C. Bonner, *Part. Fibre Toxicol.* **2020**, *17*, 60.
[31] C. M. White, R. Banks, I. Hamerton, J. F. Watts, *Prog. Org. Coat.* **2016**, *90*, 44–53.
[32] I. W. Chiang, B. E. Brinson, R. E. Smalley, J. L. Margrave, R. H. Hauge, *J. Phys. Chem. B* **2001**, *105*, 1157–1161.
[33] T. Ohta, M. Yamada, H. Kuroda, *BCSJ* **1974**, *47*, 1158–1161.
[34] M. M. Tomczyk, S. Boncel, A. Herman, T. Krawczyk, A. Jakóbik-Kolon, M. Pawlyta, M. Krzywiecki, A. Chrobak, M. Minoshima, F. Sugihara, K. Kikuchi, N. Kuźnik, *IJN* **2020**, *15*, 7433–7450.
[35] M. Suzuki, I. S. Suzuki, *Phys. Rev. B* **1998**, *58*, 371–384.
[36] K. Miyoshi, M. Hagiwara, M. Matsuura, T. Abe, Y. Mizutani, *Physica B* **1997**, *237*, 190–191.
[37] M. Suzuki, I. S. Suzuki, *Phys. Rev. B* **1998**, *58*, 371–384.
[38] M. Suzuki, I. S. Suzuki, *Phys. Rev. B* **1998**, *58*, 840–846.
[39] M. Pumera, H. Iwai, *Chemistry - An Asian Journal* **2009**, *4*, 554–560.

Entry for the Table of Contents

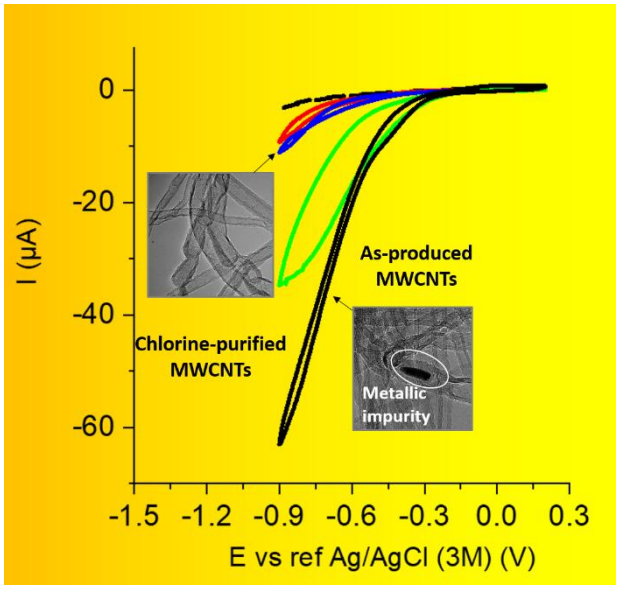

Ultra-pure MWCNTs have been prepared by means of a low energy consumption using chlorine. Unprecedented, magnetic and electrochemical measurements have been combined to ascertain the quasi complete removal of metallic impurities from MWCNt samples.